Inorganic Chemistry Research
Article

A Theoretical Study on the Strength and Nature of Metal-dithiolate Bond in Homoleptic Complexes $[M(S_2C_2R_2)_2]^{2-}$ (M=Ni(II), Pd(II), Pt(II); R=H, Me, CN)

Yasin Gholiee[a,*] and Sadegh Salehzadeh[b]

[a]*Department of Chemistry, Faculty of Science, Malayer University, Malayer, Iran*
[b]*Faculty of Chemistry, Bu-Ali Sina University, Hamedan, Iran*

Received: August 31, 2023; Accepted: October 1, 2023
Cite This: *Inorg. Chem. Res.* **2023**, *7*, 14-21. DOI: 10.22036/j10.22036.2023.414209.1151

Abstract: A theoretical study is reported on the strength and nature of metal-ligand bond in some dianionic metal-bis(dithiolate) complexes $[ML_2]^{2-}$ (M=Ni(II), Pd(II), Pt(II); L = $S_2C_2H_2^{2-}$ (edt^{2-}), $S_2C_2Me_2^{2-}$ ($dmedt^{2-}$), $S_2C_2(CN)_2^{2-}$ (mnt^{2-})). Firstly, the geometries of all complexes were optimized at the BP86 and M06 levels of theory using the def2-TZVP basis set. Then the metal-dithiolate and metal(dithiolate)-dithiolate interaction energies, the deformation energies of metal and dithiolate ions as well as the total interaction and stabilization energies of the complexes were calculated and compared. In continuation, an energy decomposition analysis (EDA) was performed to study the nature of metal-bis(dithiloate) bonds in these complexes. The results showed that among the metal complexes studied here, the Pt complexes have the largest values of interaction and stabilization energies. On the other hand, in the case of all three metal ions, the values of total interaction energies and also stabilization energies of $[M(edt)_2]^{2-}$ and $[M(dmedt)_2]^{2-}$ complexes are similar or close together and both are larger than those for $[M(mnt)_2]^{2-}$ complexes. The analysis of metal-(bis)dithiolate bonds showed that the orbital interactions are mainly Ni←Lσ interactions and have considerably less contribution to the total attractive interactions compared to electrostatic interactions.

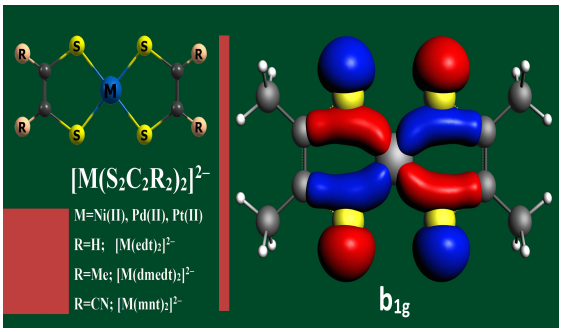

Keywords: Bis(dithiolate) complexes, Density functional theory, Energy decomposition analysis, Interaction energy, Bonding analysis

1. INTRODUCTION

Metal bis-dithiolene complexes have been extensively studied by inorganic/organic chemists in recent decades due to their several applications in the areas of conducting and magnetic molecular materials as well as their relevant optical properties.[1-6] There are three different forms with different charges for dithiolenes (see Figure 1) which make them redox-active ligands with the ability to form highly electron-delocalized complexes. However, the term dithiolene is used without taking into account the formal oxidation state of ligands to describe their noninnocent character in several metal complexes.[7] Several investigations have been carried out to explore the electronic structure of metal dithiolene complexes, using density functional theory (DFT).[5,8-13] DFT results in combination with X-ray absorption spectroscopy (XAS) data have revealed that the ligands in these species play a crucial role as electron donors or acceptors during the redox process.[14-16] Moreover, some ab initio studies have been used for predicting the singlet-triplet gap of the neutral metal dithiolene complexes.[17-20] The ionization and ultrafast dynamics of these complexes have also been studied using Photoelectron and femtosecond spectroscopies.[21-24]

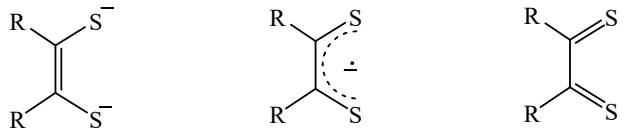

Figure 1. different forms with different charges for dithiolenes.

The homoleptic bis-dithiolene complexes of d^8 transition metals display square-planar structure and diverse forms from dianionic to cationic.[2,3] Extensive molecular orbital (MO) calculations have been carried out on four-coordinate square-planar metallo-bis(dithiolene) complexes, at different levels of theory.[25] On the other hand, it has been demonstrated in recent years that the strength of the classical chemical bondings in transition metal (TM) complexes, i.e., TM←Lσ donation and TM→Lπ back-donation, can be quantitatively assessed using energy decomposition analysis (EDA).[26-33]

This work reports a theoretical study on the strength and nature of metal-ligand bond in dianionic metal-bis(dithiolate) complexes $[M(S_2C_2R_2)_2]^{2-}$ (M=Ni(II), Pd(II), Pt(II); R=H, Me, CN). According to the Lewis formalism, the bonding in these systems (diamagnetic dianionic complexes) is summarized using the classical structure involving the metal in the 2+ oxidation state and the ligands in the ene-1,2-dithiolate form.[14] In this work, it will be focused mainly on the different types of interaction energies and the nature of metal-ligand bond. The high symmetry of the studied complexes (D_{2h}) lets us identify the orbital interactions and quantify their strength with the calculated energy decomposition analysis data. Moreover, we will attempt to determine the covalent and electrostatic character of the Metal-ligand bonds.

2. EXPERIMENTAL

Geometry optimization of all complexes were carried out at the BP86[34,35] and M06[36] levels with the def2-TZVP triple-zeta[37] basis set using the Gaussian 09[38] set of programs. The geometries of the complexes were optimized using D_{2h} symmetry. To calculate the interaction energies between the fragments in $[M(S_2C_2R_2)_2]^{2-}$ complexes, the central M^{2+} ion was considered as B fragment and two $(S_2C_2R_2)^{2-}$ ligands were considered as A and A' fragments (all in singlet states).

$$[\underbrace{(S_2C_2R_2)}_{A}\underbrace{M}_{B}\underbrace{(S_2C_2R_2)}_{A'}]^{2-}$$

The four types of IEs, between AB and A' fragments ($IE_{AB-A'}$), between A and BA' fragments ($IE_{A-BA'}$), between A and B fragments (IE_{A-B}), between B and A' fragments ($IE_{B-A'}$), were calculated using following equations:

$$IE_{AB-A'} = E^{free}_{ABA'} - \{E^{frozen}_{AB} + E^{frozen}_{A'}\} \quad (1)$$

$$IE_{A-BA'} = E^{free}_{ABA'} - \{E^{frozen}_{A} + E^{frozen}_{BA'}\} \quad (2)$$

$$IE_{A-B} = E^{frozen}_{AB} - \{E^{frozen}_{A} + E^{frozen}_{B}\} \quad (3)$$

$$IE_{B-A'} = E^{frozen}_{BA'} - \{E^{frozen}_{B} + E^{frozen}_{A'}\} \quad (4)$$

In above equations, $E^{free}_{ABA'}$ is the energy of ABA' complex in its optimized geometry. E^{frozen}_{A}, E^{frozen}_{B}, $E^{frozen}_{A'}$, E^{frozen}_{AB} and $E^{frozen}_{BA'}$ refer to the energy of A, B, A', AB and BA' frozen in the optimized geometry of ABA' system, respectively. The total interaction energy for all complexes was calculated using two different equations (5) and (6):[39–43]

$$IE_{total} = \frac{1}{2}(IE_{A-B} + IE_{B-A'} + IE_{A-BA'} + IE_{AB-A'}) \quad (5)$$

$$IE_{total} = E^{free}_{ABA'} - (E^{frozen}_{A} + E^{frozen}_{B} + E^{frozen}_{A'}) \quad (6)$$

The stabilization energies (SEs) were also calculated using the following equation:

$$SE_{ABA'} = E^{free}_{ABA'} - \{E^{free}_{A} + E^{free}_{B} + E^{free}_{A'}\} \quad (7)$$

In the above equation, E^{free}_{A}, E^{free}_{B} and $E^{free}_{A'}$ are the energies of the optimized geometry of A, B, and A' before complexation, respectively. The strain/deformation energies (DEs) of the fragments upon the formation of ABA' complexes were calculated using following equations:

$$DE_{A\ or\ B\ or\ A'} = E^{frozen\ in\ complex}_{A\ or\ B\ or\ A'} - E^{free}_{A\ or\ B\ or\ A'} \quad (8)$$

Energy Decomposition Analysis (EDA) is a popular method for quantitative interpretation of chemical bonds. Four major expressions can be interpreted from EDA calculation: the quasi-classical electrostatic interaction between two fragments, ΔE_{elstat}, the repulsive exchange or Pauli repulsion between the electrons of two fragments with the same spins, ΔE_{Pauli}, the orbital interaction or covalent character which stems from orbital relaxation and orbital mixing of two fragments, ΔE_{orb}, and the dispersion energy between two fragments (when a dispersion-corrected functional is employed), ΔE_{disp}. In such a scheme, the interaction energy (ΔE_{int}) is decomposed according to the following equation into the above-mentioned components:

$$\Delta E_{int} = \Delta E_{Pauli} + \Delta E_{elstat} + \Delta E_{orb} + \Delta E_{disp} \quad (9)$$

Energy decomposition analysis with the ADF 2013 package[44] was employed for analyzing the interaction of M^{2+} (with the electronic valence configuration: $(d_z2)^2$, $(d_{x2-y}2)^2$, $(d_{xz})^2$, $(d_{yz})^2$, $(d_{xy})^0$) and $[(S_2C_2R_2)_2]^{4-}$ (in the singlet state) in $[M(S_2C_2R_2)_2]^{2-}$ complexes at BP86/TZ2P(ZORA) level of theory.

3. RESULTS AND DISCUSSION

The optimized structures for the studied complexes, at BP86/def2-TZVP level of theory, are depicted in Figure 2, while M–S bond lengths and S–M–S bond angles are also shown on the structures. As can be seen, all complexes possess a square-planar structure around the M^{2+} ion. Among the studied complexes, $[M(mnt)_2]^{2-}$ (M=Ni(II), Pd(II), Pt(II)) and $[Ni(dmedt)_2]^{2-}$ are experimentally known and their geometries have been determined with X-ray structure analysis with D_{2h} symmetry point group.[45-48] The computed and experimental structural parameters are compared in Table S1 (see also the bold data in Figure 2). There is an excellent agreement between the experimental and calculated data. The calculated root mean squares (RMS) for bond lengths and bond angles vary from 0.029-0.037 Å and 0.1-1.8°, respectively, at BP86/def2-TZVP level of theory (from 0.030-0.043 Å and 0.2-1.8°, respectively, at M06/def2-TZVP level of theory; see Table S1).

Calculated interaction energies, between the defined fragments in the optimized structures for the studied complexes, using Eqs. (1)-(4), as well as the total interaction energies, IE_{total}, using Eqs. (5) and (6) are listed in Table 1. As can be seen, the values of IE_{total} vary from -910.1 to -968.4, -905.2 to -966.6, and -1168.9 to -1229.9 kcal/mol for Ni, Pd, and Pt complexes,

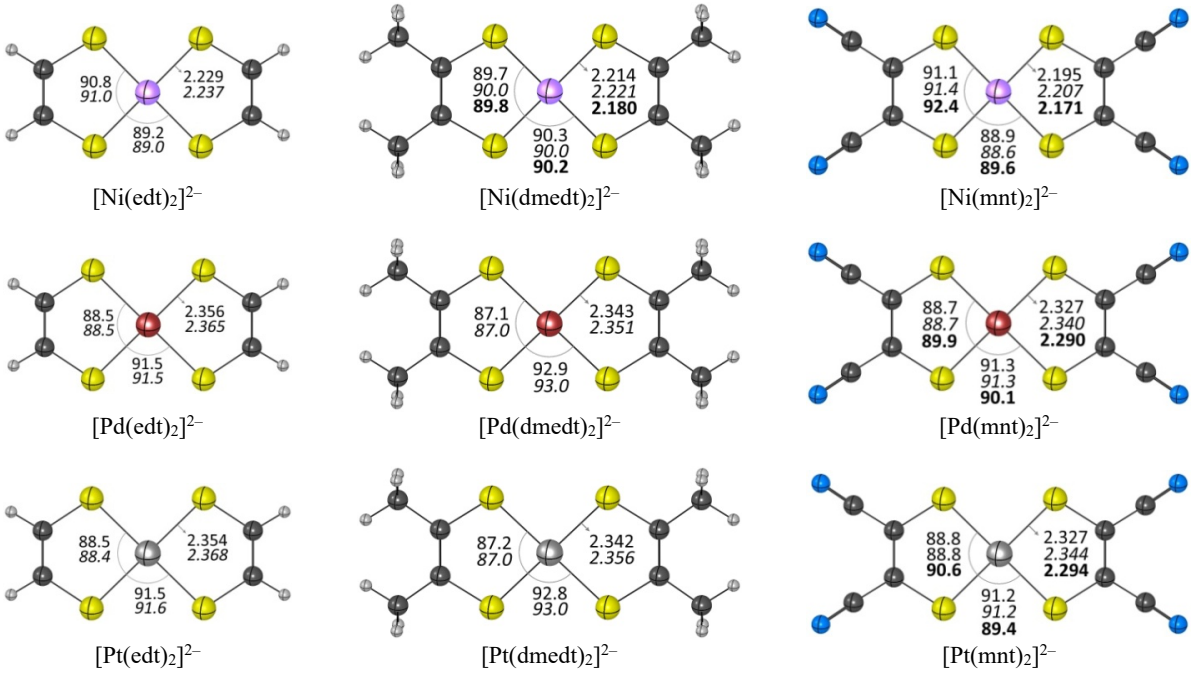

Figure 2. The optimized structures of $[ML_2]^{2-}$ (M=Ni(II), Pd(II), Pt(II); L=edt^{2-}, dmedt^{2-}, mnt^{2-}) complexes, at BP86/def2-TZVP level of theory. The calculated bond lengths (Å) and angles (°) at BP86/def2-TZVP and M06/def2-TZVP levels of theory are shown in regular and italic, respectively. The experimental data are in bold.

respectively. Moreover, in each series of $[ML_2]^{2-}$ complexes the values of IE_{total} decrease as follows: $[M(edt)_2]^{2-} > [M(dmedt)_2]^{2-} > [M(mnt)_2]^{2-}$ (see also Figure 3). It should be noted that the calculated IE_{total} values for $[M(edt)_2]^{2-}$ and $[M(dmedt)_2]^{2-}$ complexes are close together, and are larger than those for $[M(mnt)_2]^{2-}$ ones. For example, the IE_{total} values for $[Ni(edt)_2]^{2-}$, $[Ni(dmedt)_2]^{2-}$ and $[Ni(mnt)_2]^{2-}$ are -968.4, -961.9 and -910.1 kcal/mol, respectively. As it was mentioned, the studied complexes were considered as ABA' systems. So, according to Eq. (5), the strength of the bond between the components has a direct effect on the calculated total interaction energies. The data in Table 1 show that the values of $IE_{AB-A'}$ and $IE_{A-BA'}$ (interaction energy between ML fragment and the second L^{2-} ligand) in all complexes are considerably less than the values of IE_{A-B} and $IE_{B-A'}$ (interaction energy between bare M^{2+} cation and the first L^{2-} ligand). The main reason is the charge difference between the interacting fragments. The $IE_{AB-A'}$ refers to the interaction between the neutral AB and doubly negatively charged A' fragments, respectively, while the IE_{A-B} refers to the interaction between the doubly negatively charged A and doubly positively charged B fragments, respectively. Interestingly, while the calculated IE_{total} values for $[M(mnt)_2]^{2-}$ complexes are smaller than those for $[M(edt)_2]^{2-}$ and $[M(dmedt)_2]^{2-}$ ones, their $IE_{AB-A'}$ and $IE_{A-BA'}$ values are even larger than those for latter complexes. Indeed, the smaller values of IE_{total} values for $[M(mnt)_2]^{2-}$ complexes, compared to those for $[M(edt)_2]^{2-}$

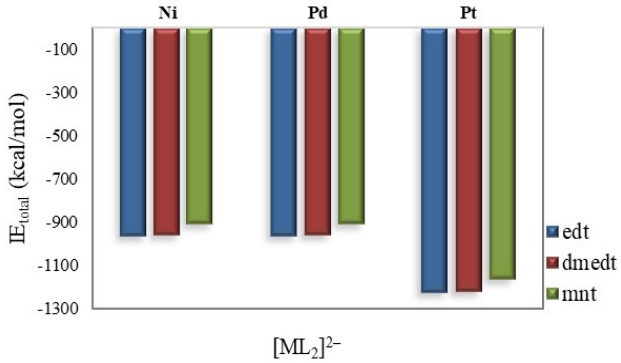

Figure 3. Variations of the calculated IE_{total} in $[ML_2]^{2-}$ (M=Ni(II), Pd(II), Pt(II); L=edt^{2-}, dmedt^{2-}, mnt^{2-}) complexes, at BP86/def2-TZVP level of theory.

and $[M(dmedt)_2]^{2-}$ ones, are the result of smaller values of IE_{A-B} and $IE_{B-A'}$. As can be seen in Table 1, for example, the $IE_{AB-A'}$ and $IE_{A-BA'}$ values for $[Ni(mnt)_2]^{2-}$ are larger than those for $[Ni(edt)_2]^{2-}$ and $[Ni(dmedt)_2]^{2-}$ (-165.2 vs -152.5 and -147.7 kcal/mol), but the values of IE_{A-B} and $IE_{B-A'}$ for $[Ni(mnt)_2]^{2-}$ are considerably smaller than those for $[Ni(edt)_2]^{2-}$ and $[Ni(dmedt)_2]^{2-}$ (-744.9 vs -814.2 and -815.9 kcal/mol). Indeed, the presence of –CN groups on the dithiolate ligands decreases the total interaction energy. It may be related to the fact that –CN substituents extend the π conjugation of the dithiolate ligand and therefore, the more electron density from the S atoms of dithiolate is tied up in ligand π conjugation rather than ligand-metal bonding.

Table 1. Calculated values of interaction energies between the fragments (IE, kcal/mol), strain/deformation energies (DE, kcal/mol) and stabilization energies (SE, kcal/mol) for $[ML_2]^{2-}$ (M=Ni(II), Pd(II), Pt(II); L=edt^{2-}, $dmedt^{2-}$, mnt^{2-}) complexes, at BP86/def2-TZVP level of theory[a]

Complexes	IE_{A-B} (=$IE_{B-A'}$)	$IE_{A-BA'}$ (=$IE_{AB-A'}$)	IE_{total} [b]	DE				SE
				A	B	A'	total	
$[Ni(edt)_2]^{2-}$	–815.9	–152.5	–968.4	11.2	70.7	11.2	93.1	–875.2
$[Ni(dmedt)_2]^{2-}$	–814.2	–147.7	–961.9	6.5	70.7	6.5	83.7	–878.1
$[Ni(mnt)_2]^{2-}$	–744.9	–165.2	–910.1	4.5	70.7	4.5	79.7	–830.3
$[Pd(edt)_2]^{2-}$	–817.9	–148.6	–966.6	7.9	53.7	7.9	69.5	–897.1
$[Pd(dmedt)_2]^{2-}$	–816.9	–143.2	–960.1	4.1	53.7	4.1	61.9	–898.2
$[Pd(mnt)_2]^{2-}$	–746.7	–158.5	–905.2	2.4	53.7	2.4	58.5	–846.7
$[Pt(edt)_2]^{2-}$	–1066.0	–163.9	–1229.9	8.1	48.3	8.1	64.5	–1165.4
$[Pt(dmedt)_2]^{2-}$	–1064.2	–158.5	–1222.7	4.0	48.3	4.0	56.3	–1166.4
$[Pt(mnt)_2]^{2-}$	–993.6	–175.3	–1168.9	2.4	48.3	2.4	53.1	–1115.8

[a]Calculated values of interaction energies (IE, kcal/mol) at the M06/def2-TZVP level are given at Table S2. [b]Equations (5) and (6) give the identical values.

The calculated strain/deformation energies (DEs) for M^{2+}, L^{2-} and L'^{2-} (B, A and A' fragments, respectively) during the formation of complexes as well as the stabilization energies (SEs) for $[ML_2]^{2-}$ complexes are also listed in Table 1. As can be seen, the calculated DE values for mnt^{2-} are smaller than those for edt^{2-} and $dmedt^{2-}$. For example, in $[NiL_2]^{2-}$ complexes, the calculated DE values for edt^{2-}, $dmedt^{2-}$ and mnt^{2-} are 11.2, 6.5 and 4.5 kcal/mol, respectively. The less structural deformation in mnt^{2-} is in agreement with the above conclusion about the extension of the π conjugation system. Indeed, the larger extension of the π conjugation on mnt^{2-} prevents more structural deformation during the formation of the complex. However, as can be seen in Table 1, the main origin of total strain/deformation energies in all studied complexes is the difference in the electronic configuration of d orbitals of M^{2+} ions before and after complexation. We note that in present square planner complexes, the M^{2+} ion is in a low spin d^8 state. Thus, as expected, the required energy for changing the ground state electronic configuration (high spin) into the low spin state will be decreased from Ni^{2+} to Pt^{2+}, because of increasing the ligand field strength.[49]

The EDA results for $[ML_2]^{2-}$ complexes are shown in Table 2. The EDA calculations have been performed using the M^{2+} ion (B fragment) with $\{L_2\}^{4-}$ ligands (AA' fragment) as interacting fragments. As can be seen, the values of the calculated ΔE_{int} for each series of $[NiL_2]^{2-}$, $[PdL_2]^{2-}$, and $[PtL_2]^{2-}$ complexes decrease from $[M(edt)_2]^{2-}$ to $[M(mnt)_2]^{2-}$. The metal-ligand bonds in all studied $[ML_2]^{2-}$ complexes possess higher electrostatic contributions (ΔE_{elstat}) toward the total attractive interactions (ΔE_{elstat} + ΔE_{orb}). Table 2 shows that the ΔE_{elstat} contributes 62.9 to 69.1% of the total attractive interactions for $Ni(dmedt)_2]^{2-}$ and $[pd(edt)_2]^{2-}$ complexes, respectively. However, the breaking down of ΔE_{orb} values into the contributions which come from orbitals belonging to different irreducible representations of the D_{2h} point group brings more insight into the orbital interactions involved between the fragments in the studied $[ML_2]^{2-}$ complexes. Table 2, also identifies the orbital symmetries with the type of metal-dithiolate orbital interactions. As can be seen, the b_{1g} orbitals, which give the M←Lσ donation of the sulfur lone-pair orbitals to the vacant d_{xy} orbital of M^{2+}, have the largest contribution to the ΔE_{orb} term (more than 50% in all studied complexes).

To gain a deeper insight into the contributions of orbital symmetries in ΔE_{orb} values, let's consider the $[Ni(dmedt)_2]^{2-}$ in which the orbital contribution is slightly more than the other studied complexes. It should be noted that the principal orientation of the complex in the Cartesian coordinate system which has been used for all complexes is shown in Figure 4. Moreover, the valence orbitals of $[Ni(dmedt)_2]^{2-}$, which provides a visual inspection of the orbital terms, are depicted in Figure 5. As can be seen in Table 2, the b_{1g} orbitals in $[Ni(dmedt)_2]^{2-}$ have 55.5% contribution to the ΔE_{orb} term. As it was mentioned, it gives the Ni←Lσ donation of the sulfur lone-pair orbitals to the vacant d_{xy} orbital of Ni^{2+}. Figure 5 shows that it comes from the $12b_{1g}$ (HOMO-10) orbital which exhibits a bonding combination between the d_{xy} atomic orbital of central metal ion and the ligand orbital. The second strongest contribution to the ΔE_{orb} term (13.3%) belongs to the a_g orbitals. The atomic orbitals that principally can participate in a_g molecular orbitals are s, d_z2 or $d_{x^2-y^2}$. As the latter atomic orbitals are doubly occupied, they can be involved only in Ni→Lσ back-donation. Figure 5 clearly shows that the $18a_g$ (HOMO-1) and $17a_g$ (HOMO-5) are mainly the filled d_z2 and $d_{x^2-y^2}$ metal orbitals, respectively, with negligible contributions from the ligand orbitals. In contrast, the

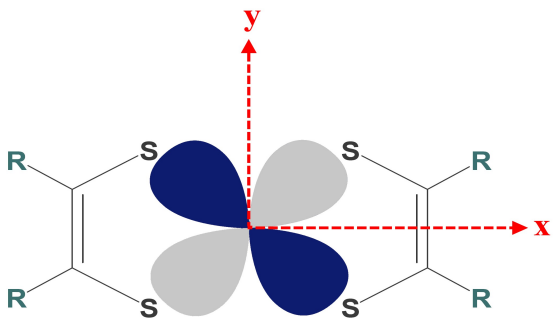

Figure 4. Orientation of the $[ML_2]^{2-}$ complexes in the cartesian coordinates (schematic view of the d_{xy} (b_{1g}) orbital of the metal ion).

Table 2. EDA results of $[ML_2]^{2-}$ (D_{2h}; M=Ni(II), Pd(II), Pt(II); L=edt^{2-}, $dmedt^{2-}$, mnt^{2-}) complexes, using M^{2+} and $\{L_2\}^{4-}$ as interacting fragments, at BP86/TZ2P(ZORA) level of theory

Complexes		**$[Ni(edt)_2]^{2-}$**	**$[Ni(dmedt)_2]^{2-}$**	**$[Ni(mnt)_2]^{2-}$**
ΔE_{int}		-1251.1	-1213.6	-1130.0
ΔE_{Pauli}		196.8	192.4	210.1
ΔE_{elatat}[a]		-990.5 (68.4%)	-884.6 (62.9%)	-847.8 (63.3%)
ΔE_{orb}[a]		-457.5 (31.6%)	-521.5 (37.1%)	-492.3 (36.7%)
$\Delta E(ag)$[b], s, d_z2, d_{x2-y2}	Ni ⇌ Lσ	-64.3 (14.1%)	-69.6 (13.3%)	-67.7 (13.8%)
$\Delta E(b_{1g})$[b], d_{xy}	Ni←Lσ	-255.6 (55.9%)	-289.6 (55.5%)	-276.4 (56.2%)
$\Delta E(b_{2g})$[b], d_{xz}	Ni→Lπ	-10.2 (2.2%)	-17.6 (3.4%)	-13.8 (2.8%)
$\Delta E(b_{3g})$[b], d_{yz}	Ni→Lπ	-7.2 (1.6%)	-5.4 (1.0%)	-4.7 (1.0%)
$\Delta E(au)$[b]	Lπ	-9.1 (2.0%)	-6.9 (1.3%)	-17.5 (3.6%)
$\Delta E(b_{1u})$[b], p_z	Ni←Lπ	-15.5 (3.4%)	-22.2 (4.3%)	-20.9 (4.2%)
$\Delta E(b_{2u})$[b], p_y	Ni←Lσ	-45.2 (9.9%)	-43.9 (8.4%)	-45.5 (9.2%)
$\Delta E(b_{3u})$[b], p_x	Ni←Lσ	-50.5 (11.0%)	-66.3 (12.7%)	-45.8 (9.3%)
		$[Pd(edt)_2]^{2-}$	**$[Pd(dmedt)_2]^{2-}$**	**$[Pd(mnt)_2]^{2-}$**
ΔE_{int}		-1230.6	-1194.6	-1108.6
ΔE_{Pauli}		272.7	258.8	282.1
ΔE_{elatat}[a]		-1039.7 (69.1%)	-930.1 (64%)	-896.4 (64.4%)
ΔE_{orb}[a]		-463.7 (30.9%)	-523.5 (36%)	-494.4 (35.6%)
$\Delta E(ag)$[b], s, d_z2, d_{x2-y2}	Pd ⇌ Lσ	-64.1 (13.8%)	-72.7 (13.9%)	-66.8 (13.6%)
$\Delta E(b_{1g})$[b], d_{xy}	Pd←Lσ	-285.7 (61.6%)	-307.1 (58.7%)	-299.0 (60.7%)
$\Delta E(b_{2g})$[b], d_{xz}	Pd→Lπ	-7.4 (1.6%)	-14.0 (2.7%)	-10.6 (2.1%)
$\Delta E(b_{3g})$[b], d_{yz}	Pd→Lπ	-7.0 (1.5%)	-5.1 (1.0%)	-8.6 (1.8%)
$\Delta E(au)$[b]	Lπ	-9.1 (2.0%)	-7.5 (1.4%)	-16.4 (3.3%)
$\Delta E(b_{1u})$[b], p_z	Pd←Lπ	-12.6 (2.7%)	-19.5 (3.7%)	-16.9 (3.4%)
$\Delta E(b_{2u})$[b], p_y	Pd←Lσ	-37.9 (8.2%)	-38.3 (7.3%)	-37.9 (7.7%)
$\Delta E(b_{3u})$[b], p_x	Pd←Lσ	-39.9 (8.6%)	-59.3 (11.3%)	-38.1 (7.7%)
		$[Pt(edt)_2]^{2-}$	**$[Pt(dmedt)_2]^{2-}$**	**$[Pt(mnt)_2]^{2-}$**
ΔE_{int}		-1262.9	-1226.7	-1141.9
ΔE_{Pauli}		358.4	339.7	369.1
ΔE_{elatat}[a]		-1108.8 (68.4%)	-993.4 (63.4%)	-965.6 (63.9%)
ΔE_{orb}[a]		-512.4 (31.6%)	-572.9 (36.6%)	-545.3 (36.1%)
$\Delta E(ag)$[b], s, d_z2, d_{x2-y2}	Pt ⇌ Lσ	-112.9 (22.0%)	-122.8 (21.4%)	-116.9 (23.7%)
$\Delta E(b_{1g})$[b], d_{xy}	Pt←Lσ	-270.4 (52.8%)	-291.3 (50.8%)	-284.2 (57.7%)
$\Delta E(b_{2g})$[b], d_{xz}	Pt→Lπ	-10.2 (2.0%)	-16.3 (2.8%)	-13.2 (2.7%)
$\Delta E(b_{3g})$[b], d_{yz}	Pt→Lπ	-9.6 (1.9%)	-7.4 (1.3%)	-10.1 (2.0%)
$\Delta E(au)$[b]	Lπ	-10.0 (2.0%)	-8.4 (1.5%)	-18.0 (3.7%)
$\Delta E(b_{1u})$[b], p_z	Pt←Lπ	-14.1 (2.8%)	-21.2 (3.7%)	-18.8 (3.8%)
$\Delta E(b_{2u})$[b], p_y	Pt←Lσ	-41.4 (8.1%)	-41.9 (7.3%)	-41.9 (8.5%)
$\Delta E(b_{3u})$[b], p_x	Pt←Lσ	-43.7 (8.5%)	-63.7 (11.1%)	-42.3 (8.6%)

[a]The percentage values in parentheses give the contribution to the total attractive interactions $\Delta E_{elstat} + \Delta E_{orb}$.[b]The percentage values in parentheses give the contribution to the total orbital interactions ΔE_{orb}.

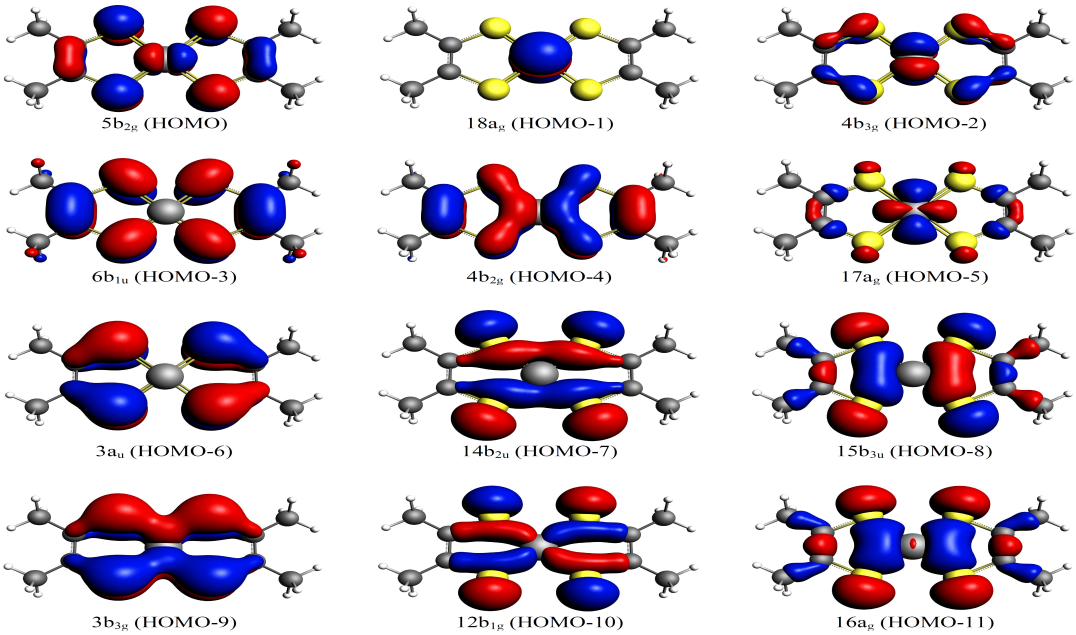

Figure 5. Plot of the highest occupied molecular orbitals of $[Ni(dmedt)_2]^{2-}$, at BP86/TZ2P(ZORA) level of theory.

16ag (HOMO-11) comes from the Ni←Lσ donation of the sulfur lone-pair orbitals into the vacant s orbital of nickel. Indeed, the Ni→Lσ backdonation is negligible and the value for $\Delta E(a_g)$ comes mainly from Ni←Lσ donation. The contribution of the b_{1u} orbitals (Ni←Lπ donation, $6b_{1u}$(HOMO-3)) provides only 4.3% of ΔE_{orb}, while the contributions of the b_{3u} and b_{2u} orbitals are 12.7% and 8.4%, respectively (Ni←Lσ donation, $15b_{3u}$(HOMO-8) and $14b_{2u}$(HOMO-7)). The $\Delta E(a_u)$ value in Table 2 gives the stabilization which only comes from the relaxation of the ligand orbital. There is no atomic orbital valence of the metal which has a_u symmetry, thus the $3a_u$(HOMO-6) orbital only has contributions from the ligand atoms. The calculated contributions of the $\Delta E(b_{2g})$ and $\Delta E(b_{3g})$ that come from the occupied d_{xz}, d_{yz} atomic orbitals of nickel (Ni→Lπ back-donation) are 3.4% and 1.0%, respectively. This means that the Ni→Lπ back-donation in $[Ni(dmedt)_2]^{2-}$ complex, and also in all other complexes, is very weak.

As was mentioned, for all studied Ni, Pd and Pt complexes, the largest contribution to the ΔE_{orb} term comes from the b_{1g} orbitals. However, the contributions of b_{1g} orbitals for the $[PdL_2]^{2-}$ complexes are larger than those in the $[NiL_2]^{2-}$ and $[PtL_2]^{2-}$ complexes. On the other hand, the next strongest contribution to ΔE_{orb} in the $[PtL_2]^{2-}$ complexes, which comes from a_g orbitals, is higher than in both the Ni and Pd complexes. The contribution of the remaining orbitals in all complexes is the same. Finally, Figure 6 demonstrates that the total interaction energies (ΔE_{int}) in each series of $[NiL_2]^{2-}$, $[PdL_2]^{2-}$ and $[PtL_2]^{2-}$ complexes do not show the same trend as ΔE_{orb} values, but the same trend as ΔE_{elstat} values ($[M(edt)_2]^{2-} > [M(dmedt)_2]^{2-} > [M(mnt)_2]^{2-}$) For example, the strongest ΔE_{int} and ΔE_{elstat} of the $[NiL_2]^{2-}$ complexes are calculated for $[Ni(edt)_2]^{2-}$ (ΔE_{int} = -1251.1 kcal/mol, ΔE_{elstat} = -990.5 kcal/mol) but the largest value for the ΔE_{orb} is calculated for $[Ni(dmedt)_2]^{2-}$ (ΔE_{orb} = -521.5 kcal/mol).

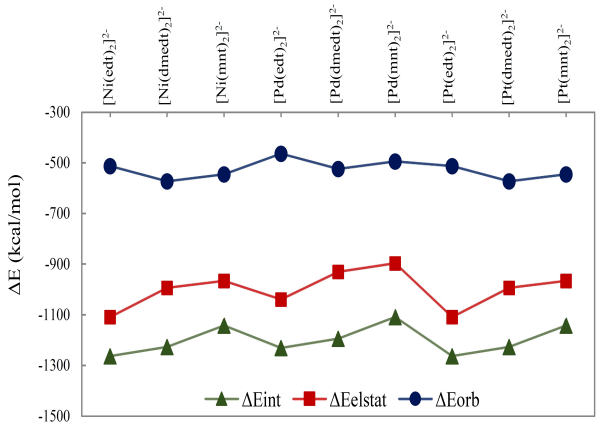

Figure 6. Trends of the ΔE_{int} and the attractive EDA terms ΔE_{elstat} and ΔE_{orb} in $[NiL_2]^{2-}$, $[PdL_2]^{2-}$ and $[PtL_2]^{2-}$ (L=edt^{2-}, dmedt^{2-}, mnt^{2-}), at BP86/TZ2P(ZORA) level of theory.

4. CONCLUSIONS

The strength and nature of metal−ligand bonds in Ni(II), Pd(II), and Pt(II) complexes of three dithiolate ligands, $S_2C_2R_2^{2-}$ (R=H, Me and CN), were studied theoretically. The results showed that the values of interaction and stabilization energies of Ni and Pd complexes studied here are close together, and both are smaller than corresponding Pt complexes. The stability of complexes depends somewhat on the type of R substituent on dithiolate ligand, and complexes with R = CN have smaller stability, compared to those with R = H or Me. The EDA calculations of the complexes also suggest that compounds with CN substituents have the weakest interaction energies ΔE_{int}, of all substituents studied in this work. The EDA data indicates that the electrostatic term ΔE_{elstat} is more important for the trend of the metal-bis(dithiolate) interactions in $[M(S_2C_2R_2)]^{2-}$ complexes than the orbital term ΔE_{orb}. The orbital interactions are mainly Ni←Lσ interactions and the contribution of both the M→Lπ and M←Lπ interactions in ΔE_{orb} are less than 4%.

CONFLICTS OF INTEREST

The authors declare that they have no known competing financial interests or personal relationships that could have appeared to influence the work reported in this paper.

ACKNOWLEDGMENTS

We are grateful to the Malayer and Bu-Ali Sina Universities for financial supports.

Appendix A. Supplementary material

Supplementary data to this article can be found online at https://doi.org/

AUTHOR INFORMATION

Corresponding Author

Yasin Gholiee: Email: yasingholiee@gmail.com, 0000-0002-0392-4407

Author

Sadegh Salehzadeh

REFERENCES

1. R. Kato, *Chem. Rev.* **2007**, *104*, 5319-5346.
2. P. Deplano, L. Pilia, D. Espa, M. L. Mercuri, A. Serpe, *Coord. Chem. Rev.* **2010**, *254*, 1434-1447.
3. B. G. Bonneval, K. I. M. Chinga, F. Alaryc, T. Bui, L. Valadea, *Coord. Chem. Rev.* **2010**, *254*, 1457-1467.
4. F. Pop, N. Avarvari, *Coord. Chem. Rev.* **2017**, *346*, 20-31.
5. T. Kusamoto, H. Nishihara, *Coord. Chem. Rev.* **2019**, *380*, 419-439.

6. J. Pitchaimani, S. F. Ni, L. Dang, *Coord. Chem. Rev.* **2020**, *420*, 213398.
7. G. Periyasamy, N. A. Burton, I. H. Hillier, M. A. Vincent, H. Disley, J. McMaster, C. D. Garner, *Faraday Discuss.* **2007**, *135*, 469-488.
8. Z. S. Herman, R. F. Kirchner, G. H. Loew, U. T. Mueller-Westerhoff, A. Nazzal, M. C. Zerner, *Inorg. Chem.* **1982**, *21*, 46-56.
9. K. Ray, S. D. George, E. I. Solomon, K. Wieghardt, F. Neese, *Chem. Eur. J.* **2007**, *13*, 2783-279.
10. F. Alarym J. L. Heully, A. Scemama, B. G. Bonneval, K. I. Chane-Ching. M. Caffarel, *Theor. Chem. Acc.* **2010**, *126*, 243-255.
11. R. Eisenberg, H. B. Gray, *Inorg. Chem*. **2011**, *50*, 9741-9751.
12. E. A. C. Bushnell, R. J. Boyd, *J. Phys. Chem. A* **2015**, *119*, 911-918.
13. A. W. Schlimgen, D. A. Mazziotti, *J. Phys. Chem. A.* **2017**, *121*, 9377-9384.
14. B. S. Lim, D. V. Fomitchev, R. H. Holm, *Inorg. Chem.* **2001**, *40*, 4257-4262.
15. S. Curreli, P. Deplano, C. Faulmann, A. Ienco, C. Mealli, M. L. Mercuri, L. Pilia, G. Pintus, A. Serpe, E. F. Trogu. *Inorg. Chem.* **2004**, *43*, 5069-5079.
16. K. Ray, A. Begum, T. Weyhermuller, S. Piligkos, J. Slageren, F. Neese, K. Wieghardt, *J. Am. Chem. Soc.* **2005**, *127*, 4403-4415.
17. D. Herebian, K. E. Wieghardt, F. Neese, *J. Am. Chem. Soc.* **2003**, *125*, 10997-11005.
18. K. Ray, T. Weyhermüller, F. Neese, K. Wieghardt, *Inorg. Chem.* **2005**, *44*, 5345-5360.
19. V. Bachler, G. Olbrich, F. Neese, K. Wieghardt, *Inorg. Chem.* **2002**, *41*, 4179-4193.
20. T. Petrenko, K. Ray, K. E. Wieghardt, F. Neese, *J. Am. Chem. Soc.* **2006**, *128*, 4422-4436.
21. T. Waters, H. K. Woo, X. B. Wang, L. S. Wang, *J. Am. Chem. Soc.* **2006**, *128*, 4282-4291.
22. T. Waters, X. B. Wang, H. K. Woo, L. S. Wang, *Inorg. Chem.* **2006**, *45*, 5841-5851.
23. X. Liu, G. L. Hou, X. Wang, X. B. Wang, *J. Phys. Chem. A* **2016**, *120*, 2854-2862.
24. V. F. Plyusnin, I. P. Pozdnyakov, V. P. Grivin, A. I. Solovyev, H. Lemmetyinen, N. V. Tkachenko, S. V. Larionov, *Dalton Trans.* **2014**, *43*, 17766-17774.
25. M. L. Kirk, R. L. McNaughton, M. E. Helton, The Electronic Structure and Spectroscopy of Metallo-Dithiolene Complexes. In: Progress in Inorganic Chemistry, E.I. Stiefel, John Wiley & Sons, Inc. **2003**, Vol. 52.
26. K. K. Pandey, M. Lein, G. Frenking, *J. Am. Chem. Soc.* **2003**, *125*, 1660-1668.
27. A. Krapp, K. K. Pandey, G. Frenking, *J. Am. Chem. Soc.* **2007**, *129*, 7596-7610.
28. G. F. Caramori, G. Frenking, *Organometallics*. **2007**, *26*, 5815-5825.
29. S. Erhardt, G. Frenking, *J. Organomet. Chem.* **2009**, *694*, 1091-1100.
30. G. F. Caramori, G. Frenking, *Theor. Chem. Acc.* **2008**, *120*, 351-361.
31. G. Prabusankar, C. Gemel, P. Parameswaran, C. Flener, G. Frenking, R. A. Fischer, *Angew. Chem., Int. Ed.* **2009**, *48*, 5526-5529.
32. J. A. Gámez, R. Tonner, G. Frenking, *Organometallics* **2010**, *29*, 5676-5680.
33. M. Bayat, M. Hopffgarten, S. Salehzadeh, G, Frenking, *J. Organomet. Chem.* **2011**, *696*, 2976-2984.
34. A. D. Becke, *Phys. Rev. A* **1988**, *38*, 3098-3100.
35. J. D. Perdew, *Phys. Rev. B* **1986**, *33*, 8822-8824.
36. Y. Zhao, D. G. Truhlar, Theor. Chem. Acc. **2008**, *120*, 215-241.
37. F. Weigend, R. Ahlrichs, *Phys. Chem. Chem. Phys.* **2005**, *7*, 3297-3305.
38. M. J. Frisch, G. W. Trucks, H. B. Schlegel, G. E. Scuseria, M. A. Robb, J. R. Cheeseman, G. Scalmani, V. Barone, B. Mennucci, G. A. Petersson, H. Nakatsuji, M. Caricato, X. Li, H. P. Hratchian, A. F. Izmaylov, J. Bloino, G. Zheng, J. L. Sonnenberg, M. Hada, M. Ehara, K. Toyota, R. Fukuda, J. Hasegawa, M. Ishida, T. Nakajima, Y. Honda, O. Kitao, H. Nakai, T. Vreven, J. A. Montgomery, Jr., J. E. Peralta, F. Ogliaro, M. Bearpark, J. J. Heyd, E. Brothers, K. N. Kudin, V. N. Staroverov, R. Kobayashi, J. Normand, K. Raghavachari, A. Rendell, J. C. Burant, S. S. Iyengar, J. Tomasi, M. Cossi, N. Rega, J. M. Millam, M. Klene, J. E. Knox, J. B. Cross, V. Bakken, C. Adamo, J. Jaramillo, R. Gomperts, R. E. Stratmann, O. Yazyev, A. J. Austin, R. Cammi, C. Pomelli, J. W. Ochterski, R. L. Martin, K. Morokuma, V. G. Zakrzewski, G. A. Voth, P. Salvador, J. J. Dannenberg, S. Dapprich, A. D. Daniels, O. Farkas, J. B. Foresman, J. V. Ortiz, J. Cioslowski and D. J. Fox. Inc., Wallingford CT., **2009**.
39. S. Salehzadeh, F. Maleki, *J. Comput. Chem.* **2016**, *37*, 2799-2807.
40. Y. Gholiee, S. Salehzadeh, S. Khodaveisi, *New J. Chem.* **2019**, *43*, 7797-7805.
41. S. Hokmi, S. Salehzadeh, Y. Gholiee, *J. Comput. Chem.* **2021**, *42*, 1354-1363.
42. Z. Nassery-Thekyeh, Y. Gholiee, *Comput. Theor. Chem.* **2022**, *1215*, 113814.
43. S. Hokmi, S. Salehzadeh, Y. Gholiee, *New J. Chem.* **2022**, *46*, 2678-2686.
44. G. Frenking, F. M. Bickelhaupt, The EDA perspective of chemical bonding. In: The Chemical Bond: Fundamental Aspects of Chemical Bonding, Wiley-VCH, Weinheim, **2014**, Vol. 1, pp. 121-158.
45. J. R. Zhou, C. L. Ni, L. L. Yu, *Acta Cryst.* **2007**, *63*, 1427-1429.

46. V. Madhu, S. K. Das, *Eur. J. Inorg. Chem.* **2006**, *2006*, 1505-1514.
47. D. Espa, L. Pilia, L. Marchiò, M. L. Mercuri, A. Serpe, E. Sessinia, P. Deplano, *Dalton Trans.* **2013**, *42*, 12429-12439.
48. B. S. Lim, D. V. Fomitchev, R. H. Holm, *Inorg. Chem.* **2001**, *40*, 4257-4262.
49. C. K. Jørgensen, Modern aspects of ligand field theory. Amsterdam, London: North-Holland, American Elsevier, New York, **1971**.